that bursts of sporadic radio emission and noise storms of varying duration and intensity occur in the centimeter and decimeter bands. Bursts and noise storms of global nature are encountered. During the time from September 1970 through November 1972 (150 observing days), 5800 bursts were registered at $\lambda = 50$ cm and 1900 at other wavelengths. There were 25 noise storms lasting more than an hour at 50 cm, and 650 lasting longer than 10 minutes. Among all of the bursts at the 50-cm wavelength, there were about 400 double and 130 triple coincidences. No similarities of form were observed between any of the observed bursts. This means that they are of near-earth origin and do not come from the remote cosmos. The generation phenomenon occurs either at great heights, on the order of several thousand kilometers (the height from which the Crimea and Ussuriĭsk are simultaneously visible), or at heights in the hundreds of kilometers, in which case the generation region would cover a wide area. Figure 1 shows the diurnal variation of the experimental and probable number densities of coinciding bursts, $\bar{n}_2$ (hr^{-1}). The figure shows morning and evening density maxima on the diurnal curve of burst coincidences at different stations, resembling the maxima in the diurnal curve of magnetic disturbances. Bursts coincide at three stations only during the day. The most probable cause of the sporadic radio emission may be generation in the earth's ionomagnetosphere due to the various corpuscular streams incoming from the sun and from the radiation belts.

The statistical characteristics of the bursts were studied (length and intensity distributions, diurnal variation, etc.). It was shown that the average duration of the bursts varies from 0.5 to 4.5 min, depends on the epoch of the observations, and does not depend on the wavelength or the place of the observations. The monthly average single-burst densities $\bar{n}_1$ and the densities of double and triple burst coincidences $\bar{n}_2$ and $\bar{n}_3$ depend on the epoch of the observations, although this dependence was not observed for the average intensity of the bursts. The monthly average burst density increases in proportion to wavelength over the entire wavelength range from 3 to 50 cm. The radiation in the bursts is partially polarized, and they have spectral widths of 0.02 to 1 GHz. The average intensity of the bursts referred to the brightness temperature of the sky is 40–50°K, which gives a radiant flux of $(3-5)\times 10^{21}$ W/m^{2}Hz. The analysis given in[8] indicated that the coefficients of correlation of the monthly average density of single and coinciding bursts and noise storms with the monthly average areas of sunspots and chromospheric flares are the same, ranging from 0.75 to 0.85. Thus, the entire set of properties of the bursts and noise storms of background sporadic radio emission indicates a statistical relation to the solar activity indices. This is illustrated graphically in Fig. 2, which shows plots obtained from the time dependences $\bar{n}_1(t)$, $\bar{n}_2(t)$ and $\bar{S}_P(t)$, $\bar{S}_F(t)$ for the monthly average density $\bar{n}_1$ of single flares as a function of the monthly average areas of sunspots and chromospheric flares for the entire period of the observations, which spans an appreciable part of the 11-year solar activity cycle; various sporadic radio emission mechanisms were considered.

Bursts of the background radio emission were compared with the dates of 16 γ-radiation bursts during 1970–1972. It was found that simultaneous observations were made on only one day, 30 June 1971. On this day, synchronous observations of the radio emission was

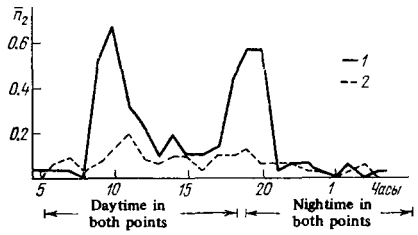

FIG. 1. Diurnal trends of actual and probable densities of double Gor'kiĭ-Crimea coincidences, averaged over the period from September 1 to November 2, 1970 ($\lambda = 50$ cm). 1—Actual number of coincidences; 2—random number of coincidences.

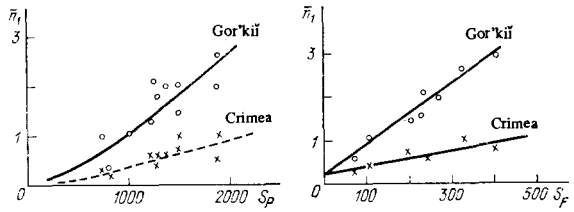

FIG. 2. Monthly average density of single bursts $\bar{n}_1$ as a function of sunspot area and chromospheric-flare area in 1970-1972 for the Crimea and Gor'kiĭ ($\lambda = 50$ cm).

made at Gor'kiĭ and in the Crimea at wavelengths of 20, 35, and 50 cm. It does not seem accidental that a radio burst was observed in the Crimea at $20^h29^m30^s$ Moscow Time on precisely this day, anticipating a γ-radiation burst by 30 seconds. The burst had an effective temperature of 8°K, which corresponds to a flux of $5\cdot 10^{-22}$ W/m^2; the burst lasted for 20 seconds and was bell-shaped. No bursts were observed at around that time either at Gor'kiĭ or in the Crimea, either at 50 cm or at any of the other wavelengths. The Galactic center was on the local horizon for the observations in the Crimea, but below the horizon at Gor'kiĭ.

The bursts of sporadic radio emission from near-earth space that we observed are capable of masking cosmic pulses strongly, making it difficult to observe them. From this standpoint, the centimeter band is the most suitable one for observations of radio-emission pulses.

[1] W. N. Charman, J. H. Fruin and J. V. Jelley, Nature **232** (5307) (1971).
[2] R. B. Partridge and G. T. Wrixon, Astrophys. J. **173** (2, pt. 1) (1972).
[3] R. B. Partridge, Phys. Rev. Lett. **26** (15) (1971).
[4] V. A. Hughes and D. S. Retallack, Nature **242** (5393) (1973).
[5] V. B. Braginskiĭ, A. B. Manukin, E. I. Popov, V. N. Rudenko, and A. A. Khorev, Usp. Fiz. Nauk 108, 595 (1972) [Sov. Phys.-Uspekhi 15, 436 (1973)].
[6] G. A. Baird and M. A. Pomerantz, Phys. Rev. Lett. **28**, 1337 (1972).
[7] V. S. Troitskiĭ, L. N. Bondar', A. M. Starodubtsev, et al., Izv. Vuzov (Radiofizika) **16** (3) (1973).
[8] V. S. Troitskiĭ, L. N. Bondar', A. M. Starodubtsev, et al., Dokl. Akad. Nauk SSSR **212** (3) (1973) [Sov. Phys.-Dokl. 18 (11) (1974)].

F. Yu. Aliev and É. G. Kasumova. Thermal-Expansion and Electric-Conductivity Anomalies in Cooled $CuFeS_2$ Films. The thermal expansion and electric conductivity of semiconductor films of complex composition have been under investigation for a number of years with the

purpose of studying the influence of quantization of carrier energy levels[1] and casting light on certain properties of this state of matter. Early studies of CuS films at low temperatures resulted in the observation of a new property—temperature oscillations of electric conductivity and the temperature coefficient of expansion (TCE). This effect is governed by shifting of quantized levels (subbands) with respect to the chemical-potential level, which was first referred to as the quantum temperature size effect (QTSE) in[2] and conforms to the theory of[3].

It was also established that the temperature of the superconductive transition is higher in a CuS film (T_c = 1.65°K for a bulky specimen and ~3°K for the film)[4]. These investigations and theoretical premises[5] pointed to the possibility of superconductivity in quantizing films of semiconductors with relatively high transition temperatures. To this end, we investigated thermal expansion and electric conductivity in films of the antiferromagnetic semiconductor $CuFeS_2$ from 2 to 300°K.

It was noted during preparation of the films that significant differences appear in their properties depending on the condensation method. The films were prepared by thermal vaporization of the compound $CuFeS_2$ in a vacuum of $\sim 5 \cdot 10^{-5}$ mm Hg with the surface of the base positioned parallel and perpendicular to the axis of the conical tungsten vaporizer. Thermal expansion was measured in the range from 4.2 to 300°K by the double-helix method[6].

Figure 1 shows a plot of the difference between the relative length changes of the specimen and glass in units of the instrument's sensitivity $S_T = 8.3 \cdot 10^{-7}$ for a film ~200 Å thick. We see that an anomaly is observed, i.e., the linear thermal expansion decreases and oscillates as the temperature is raised. Figure 2 shows the TCE as a function of temperature, the curve having been obtained by differentiating the above curve for the $CuFeS_2$ film ~200 Å thick with consideration of the expansion of the glass. It is seen that the TCE assumes negative values in certain temperature ranges between 4.2 and 89°, and that a QTSE whose amplitude increases exponentially with temperature is observed[3].

At 89°K, the TCE has a discontinuity similar to a second-order phase transition. Another occurs in the range 240–280°K, apparently due to an antiferromagnetic transformation.

A similar picture was also obtained for a film ~400 Å thick, where the transition occurs around 79°K. To establish the nature of the transition at 90°K, we also measured the electric conductivities of $CuFeS_2$ films down to 2°K. Figure 3 shows a plot of the resistivity ρ against temperature for a film of thickness ~200 Å that had been deposited on a flat glass base by parallel displacement of the base around the vaporizer. As we see, the temperature oscillation of ρ is clearly in evidence in this case up to 88°K, where resistivity is observed to "vanish" in a narrow temperature range about 2° wide. Here the resistivity drops from 483 to 12 Ω, i.e., by a factor of approximately 40; at the higher edge of the dip, the resistivity is $\sim 2.42 \cdot 10^{-3}$ Ω·cm, and at the lower edge $\sim 6 \cdot 10^{-5}$ Ω·cm. Above 90°K, resistivity is abruptly restored and the previous trend of the ρ-T dependence continues.

A similar picture is obtained for films ~500 Å thick, with the difference that the transition temperature decreases to 70.2°K and the dip narrows to ~0.7°.

In the case of perpendicular condensation, the resistivity takes a semiconductor-like trend with no distinctive features, as in a bulky specimen. It is interesting to note that the above phenomena—the jump in resistivity and the TCE—are observed in films in which a QTSE occurs. The choice of such a substance was dictated by the fact that $CuFeS_2$ is a mixture of two ionic states, $Cu^1 + Fe^3 + S_2^{2-}$ and $Cu^2 + Fe^2 + S_2^{2-}$, with ionic and covalent bonds, which result in the participation of various electron groups in the kinetic and thermodynamic properties. The fact that "vanishing" of resistivity at 89°K and the second-order phase transition, defined by the TCE jump, were observed in the films permits the statement that this transition is a superconductive transition

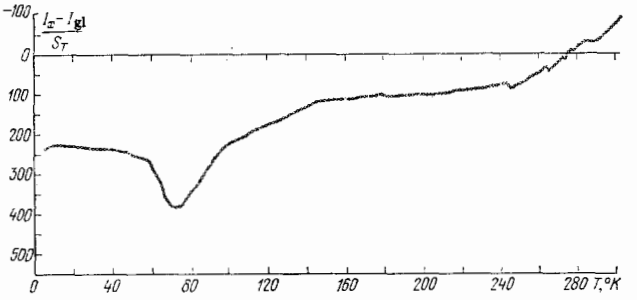

FIG. 1. Difference between relative length changes of the specimen and glass plotted against temperature in units of instrument sensitivity $S_T = 8.3 \times 10^{-7}$ for a $CuFeS_2$ film ~200 Å thick.

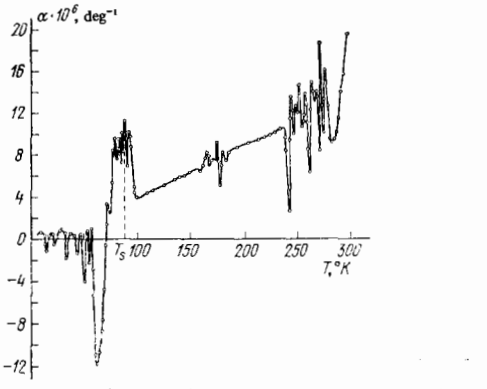

FIG. 2. Temperature coefficient of expansion vs. temperature for $CuFeS_2$ film ~200 Å thick.

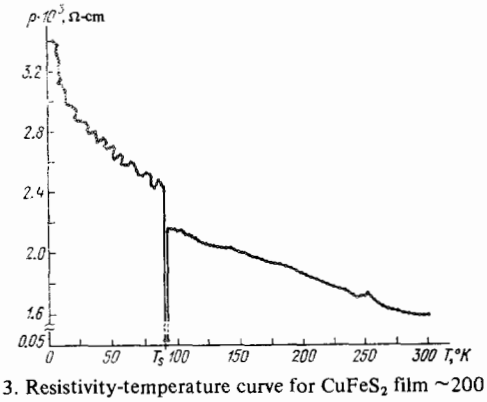

FIG. 3. Resistivity-temperature curve for $CuFeS_2$ film ~200 Å thick.

due to Coulomb interaction of electrons of different groups in accordance with the theory of [5].

According to this theory, the transition is effected in a limited temperature range above and below which the superconductor is in the normal state. The observed effect is highly complex in nature, since it involves, in addition to the mechanism indicated, an evidently important contribution from magnetic-property anisotropy, depending on film-condensation conditions, and the increase in the transition temperature is governed partly by exchange interaction of electrons of different groups, to which attention was drawn earlier in [7].

The appearance of residual resistivity and oscillation of the TCE in the neighborhood of the transition point are evidently connected by correlation of the state-density fluctuations of the different electron groups.

The material of the paper was published in ZhETF Pis. Red. 18, 3 (1973) [JETP Lett. 18, 1 (1973)].

[1] B. A. Tavger and V. Ya. Demikhovskiĭ, Usp. Fiz. Nauk 96, 61 (1968) [Sov. Phys.-Uspekhi 11, 64 (1968)].
[2] F. Yu. Aliev, F. R. Godzhaev, I. G. Kerimov, and E. S. Krupnikov, ZhETF Pis. Red. 13, 679 (1971); 15, 24 (1972) [JETP Lett. 13, 480 (1971); 15, 16 (1972)].
[3] S. S. Nedorezov, Zh. Eksp. Teor. Fiz. 59, 1353 (1970) [Sov. Phys.-JETP 32, 739 (1971)].
[4] F. Yu. Aliev, I. G. Kerimov, F. R. Godzhaev, E. I. Kalinina, and E. S. Krupnikov, Dokl. Akad. Nauk Azerb. SSR 27 (9), 18 (1971).
[5] V. Z. Kresin and B. A. Tavger, Fiz. Tverd. Tela 8, 1008 (1966) [Sov. Phys.-Solid State 8, 808 (1966)].
[6] B. G. Lazarev and A. I. Sudovtsov, Dokl. Akad. Nauk SSSR 69, 345 (1949).
[7] V. L. Ginzburg, Zh. Eksp. Teor. Fiz. 31, 202 (1956) [Sov. Phys.-JETP 4, 153 (1957)]; S. V. Vonsovskiĭ and M. S. Svirskiĭ, Dokl. Akad. Nauk SSSR, 122, 204 (1958) [Sov. Phys.-Dokl. 3, 949 (1958)]; Zh. Eksp. Teor. Fiz. 39, 384 (1960) [Sov. Phys.-JETP 12, 272 (1961)].

N. E. Alekseevskiĭ and A. A. Slutskin. Magnetic Breakdown in Metals. The intensities of the magnetic fields used in contemporary experiments to study the low-temperature properties of metals usually conform closely to the quasiclassicism condition $\kappa = \hbar\omega_c/\epsilon_F \ll 1$ (ω_c is the characteristic cyclotron frequency and ϵ_F is the Fermi energy). As we know, this inequality has made it possible to explain many experimental results in terms of classical motion of a conduction electron on orbits in momentum space.

But it has recently become clear that a whole series of experimental facts do not fit within the framework of the classical scheme. To explain them, it is necessary to take account of the quantum nature of conduction-electron dynamics even in the zeroth approximation in the quasiclassicism parameter κ. These anomalies are due to magnetic breakdown (MB)[1]—interband tunneling transitions of conduction electrons that occur in sufficiently strong magnetic fields in narrow regions of momentum space with small interband energy gaps.

The principal dynamic characteristic of magnetic breakdown is the probability of interband tunneling $W = \exp(-H_0/H)$, where the constant $H_0 = (m_0 c/e\hbar)\Delta^2/\epsilon_F$ (m_0 is the mass of the free electron, c is the velocity of light, Δ is the interband energy gap in the magnetic-breakdown region, and e is the electronic charge). In the limit $W \to 1$, $H \gg H_0$, magnetic breakdown causes only topological restructuring of the classical orbits, i.e., this limiting situation (just as in the case of weak breakdown, $W \to 0$, $H_0 \gg H$) can be treated classically. It was shown in[2] that a fundamentally different quantum limit picture appears in the intermediate field range $H \sim H_0$, $W(1-W) \sim 1$. At these values of H, kinetic phenomena in metals exhibit a kind of duality that reflects the corpuscular-wave dualism of the magnetic-breakdown dynamics of the conduction electrons. It is found[2] that two qualitatively different approaches are possible in the interpretation of experimental data on magnetic breakdown. In one of them (the stochastic approach), the electrons are regarded as classical particles that "skip" between orbits at random with a probability W in the magnetic-breakdown regions. In the other approach, the electron is regarded as a wave for which the magnetic-breakdown region is a semitransparent tunnel contact. The wave passes through this contact with an amplitude equal to $\sqrt{W}$. Since the various reflected and transmitted waves interfere coherently with one another, the kinetic coefficients of magnetic breakdown are found to be very sensitive to the phase of the electron wave function.

According to[2], which of these mutually complementary cases develops is determined by the presence of large-scale weak deformation fields created in the metal by extended defects of the dislocation type. If the concentration of these defects is high enough, quantum coherence is disturbed and a transition to the stochastic case occurs.* Inhomogeneity of the external magnetic field may also give rise to a similar stochastization. It must be stressed that the dualism described here occurs only under magnetic-breakdown conditions.

The above aspects are particularly conspicuous in the behavior of the magnetic susceptibility tensor $\rho_{ik}(H)$. We studied the susceptibilities of Nb and Be experimentally. The measurements were made in a solenoid, either superconductive or water-cooled, that created a field of 150 kOe. Use of magnetic concentrators made it possible to perform measurements in fields up to 180 kOe with sufficiently high field homogeneity.

1. Magnetic breakdown in Nb[3]. Highly perfect specimens of Nb with $\rho(300^\circ K)/\rho(4.2^\circ K)_{H=0} = 10^5$ and a dislocation density $\approx 10^4$ cm^{-2} were used for the measurements. Figure 1 shows the characteristic $\rho_{xx}(H)$ curve. It shows that $\rho_{xx}(H)$ reaches saturation. For metallic Nb with an open surface in the third zone and $n_1 \neq n_2$, this definitely indicates the intervention of magnetic breakdown. Analysis of the data showed good agreement between the experiment and the "coherent" theory. And this should be expected in view of the perfection of the Nb specimens. Comparison of theory with the experiment showed that the breakdown field $H_0 = 280 \pm 20$ kOe and that the interband gap $\Delta \approx 0.09$ eV (0.0068 rydberg). The value obtained for Δ agrees with theoretical conceptions[4] as to the electronic spectrum of Nb.

2. Magnetic breakdown in Be was observed in[5] from the break on the $\rho(H)$ curve. It was later shown in[6] that magnetic breakdown in Be between the small "cigar" orbit and the large "corona" orbit is accompanied by giant oscillations of $\rho(H)$ (Fig. 2) that are periodic in $1/H$ with period $e\hbar/cS$, where S is the area of the small orbit. The relative amplitude A of the oscillations was ~ 1, indicating that they are of "coherent" origin and fundamentally different from all hitherto known oscilla-